Comprehensive Molecular Profiling of Sinonasal Teratocarcinosarcoma Highlights Recurrent SMARCA4 Inactivation and CTNNB1 Mutations

Lisa M. Rooper, MD,† Abbas Agaimy, MD,‡ Jeffrey Gagan, MD, PhD,§ Roderick H.W. Simpson, MB, ChB, FRCPath,‖ Lester D.R. Thompson, MD,¶ Anna M. Trzcinska, DMD,# Nasir Ud Din, MBBS,** and Justin A. Bishop, MD§*

Abstract: Sinonasal teratocarcinosarcoma (TCS) is a rare tumor defined by intermixed neuroepithelial, mesenchymal, and epithelial elements. While its etiology was historically ambiguous, we recently reported frequent SMARCA4 loss by immunohistochemistry, suggesting that TCS might be related to SMARCA4-deficient sinonasal carcinomas. However, other molecular alterations including *CTNNB1* mutation have been reported in TCS, and its full genetic underpinnings are unclear. Here, we performed the first comprehensive molecular analysis of sinonasal TCS to better understand its pathogenesis and classification. We collected 30 TCS including 22 cases from our initial study. Immunohistochemical loss of SMARCA4 was seen in 22 cases (73%), with total loss in 18 cases (60%). β-catenin showed nuclear localization in 14 cases (64%) of the subset tested. We selected 17 TCS for next-generation sequencing with enrichment for partial or intact SMARCA4 immunoexpression. We identified inactivating *SMARCA4* mutations in 11 cases (65%) and activating *CTNNB1* mutations in 6 cases (35%), including 5 cases with both. Of 5 cases that lacked *SMARCA4* or *CTNNB1* mutation, 2 harbored other SWI/SNF complex and Wnt pathway alterations, including 1 with *SMARCB1* inactivation and 1 with concomitant *APC* and *ARID1A* mutations, and 3 had other findings, including *DICER1* hotspot mutation. These findings confirm that *SMARCA4* inactivation is the dominant genetic event in sinonasal TCS with frequent simultaneous *CTNNB1* mutations. They further underscore a possible relationship between TCS and sinonasal carcinomas with neuroendocrine/neuroectodermal differentiation. However, while SMARCA4 and β-catenin immunohistochemistry may help confirm a challenging diagnosis, TCS should not be regarded as a molecularly defined entity.

Key Words: nasal neoplasms, nasal cancers, malignant teratocarcinosarcoma, *SMARCA4*, BRG1, *CTNNB1*, β-catenin, immunohistochemistry, molecular diagnostics

(*Am J Surg Pathol* 2022;00:000–000)

BACKGROUND

Sinonasal teratocarcinosarcoma (TCS) is a rare and aggressive sinonasal tumor that is defined by the presence of intermixed neuroepithelial, mesenchymal, and epithelial components.[1,2] Historically, the etiology of sinonasal TCS has been unclear, with competing hypotheses suggesting true germ cell derivation, origin from pluripotent stem cells in the olfactory membrane, and divergent differentiation in a high-grade neuroectodermal tumor.[3–7] Recently, our group reported recurrent immunohistochemical (IHC) loss of SMARCA4 in 82% of TCS, including 68% that showed complete loss and 14% with partial expression.[8] We confirmed biallelic *SMARCA4* inactivation at the molecular level in 3 cases that had complete IHC loss. These findings suggested that TCS is a somatic malignancy that may be on a spectrum with the recently described SMARCA4-deficient sinonasal carcinoma. Consequently, TCS has been classified in the sinonasal carcinoma category in the Fifth Edition WHO Classification of Head and Neck Tumours.[1]

Despite the predominance of SMARCA4 loss in our previous publication, rare cases of TCS have been reported that have alternate molecular findings. Birkeland and colleagues reported an activating *CTNNB1* mutation in 1 case and Belardinilli and colleagues reported a *PIK3CA* mutation in 1 case.[9,10] Furthermore, loss of SMARCA4 was not a uniform feature across the tumors in our previous study, with 18% of cases showing intact IHC expression. In addition, our group recently reported 2 cases that showed close histologic similarities to TCS but harbored the *NAB2::STAT6* fusion considered pathognomonic of

From the Departments of *Pathology; †Oncology, The Johns Hopkins University School of Medicine, Baltimore, MD; ‡Institute of Pathology, Friedrich-Alexander-University Erlangen-Nürnberg, University Hospital, Erlangen, Germany; §Department of Pathology, University of Texas Southwestern Medical Center, Dallas, TX; ‖Department of Anatomical Pathology, University of Calgary, Calgary, AB, Canada; ¶Head and Neck Pathology Consultations, Woodland Hills, CA; #Department of Pathology, University Hospitals, Cleveland, OH; and **Department of Pathology and Laboratory Medicine, Aga Khan University, Karachi, Pakistan.

A portion of this data was presented in abstract form at the 2021 USCAP Virtual Annual Meeting.

Supported in part by the Jane B. and Edwin P. Jenevein, MD Endowment for Pathology at UT Southwestern Medical Center.

Conflicts of Interest and Source of Funding: The authors have disclosed that they have no significant relationships with, or financial interest in, any commercial companies pertaining to this article.

Correspondence: Justin A. Bishop, MD, University of Texas Southwestern Medical Center, 6201 Harry Hines Boulevard, Dallas, TX 75390-9073 (e-mail: justin.bishop@utsouthwestern.edu).

solitary fibrous tumor.[11] While these findings suggest that the histologic category of TCS may be driven by a diverse range of genetic events, the full molecular spectrum of TCS has never been systematically evaluated. In this study, we sought to perform comprehensive molecular profiling of a large group of sinonasal TCS with known SMARCA4 IHC status to more fully assess their genetic underpinnings and better understand their pathogenesis and classification.

METHODS

Case Selection

We identified a total of 30 cases of sinonasal TCS from the authors' surgical pathology archives and consultation files. This included 22 cases that were included in our previous study[8] and 8 cases that were identified subsequently. All available histologic sections were reviewed for initial inclusion in the cohort by at least 2 expert head and neck pathologists, and the diagnosis of TCS was confirmed on the basis of intermixed neuroepithelial, mesenchymal, and epithelial elements. Additional detailed histologic review was subsequently performed on 25 cases that still had hematoxylin and eosin sections available at the time of this follow-up study, and the various histologic components of the tumors were tabulated in detail. The frequency of histologic features was compared via Fisher exact test with a significance level set at 0.05 using the statistical programming language R (R Foundation, Vienna, Austria).

Immunohistochemistry

We performed IHC on all 30 cases of TCS using a mouse monoclonal antibody for SMARCA4 (clone EPNCIR111A; Abcam, Cambridge, MA; 1:00 dilution). We also performed IHC on additional TCS cases that had sufficient tumor tissue available using mouse monoclonal antibodies for SMARCB1 (clone 25/BAF47; BD Pharmingen, San Diego, CA; 1:00 dilution) and β-catenin (clone 14; BD Biosciences, Franklin Lakes, NJ; 1:1000 dilution). In brief, we cut whole-slide sections of formalin-fixed paraffin-embedded tissue blocks at 4 μM thickness. We then performed antigen retrieval and staining on Ventana BenchMark Ultra autostainers (Ventana Medical Systems, Tucson, AZ) using standardized automated protocols in the presence of appropriate controls. We visualized signals via the ultraView polymer detection kit (Ventana Medical Systems).

Next-generation Sequencing

In addition to the 3 cases of sinonasal TCS that underwent molecular analysis in our previous study, 14 additional cases with sufficient tissue available were also selected for molecular analysis. Tumors with partial or intact SMARCA4 immunoexpression were prioritized for sequencing to capture the full molecular spectrum of TCS. We performed targeted next-generation sequencing (NGS) on these cases as previously described.[12] In short, we isolated DNA using Qiagen AllPrep kits (Qiagen, Germantown, MD). We then used custom NimbleGen probes (Roche, Indianapolis, IN) to create an enriched library containing all exons from >1425 cancer-related gene. Finally, we performed sequencing on a NextSeq. 550 (Illumina, San Diego, CA) with a median 900× target exon coverage. For all cases, we reviewed variants using the Integrated Genomics Viewer (Broad Institute, Cambridge, MA) and annotated using the gnomAD and dbSNP databases.

RESULTS

Clinical and Demographic Information

The 30 sinonasal TCS affected 18 men and 12 women with a median age of 50 years (range: 18 to 79 y). There were 25 tumors (83%) centered in the superior aspect of the nasal cavity, 2 (7%) in the ethmoid sinus, 2 (7%) in the maxillary sinus, and 1 (3%) in the mastoid, although most tumors presented at high stage with extension to multiple sinonasal subsites and extensive skull base involvement. Tumors had a median size of 5.8 cm (range: 1.2 to 10.1 cm). Because many of the tumors were seen in consultation, treatment and follow-up information was not available beyond what was reported in our previous series.[8]

Histologic Findings

By far, neuroepithelial elements were the most common components of the TCS, comprising the dominant differentiation in 16 cases (64%). Immature neuroepithelial tissue was present in all cases, with intermixed mature areas in 8 (32%). The immature elements included nests and sheets of primitive cells with scant amphophilic cytoplasm and indistinct borders (Fig. 1A). They comprised the most overtly malignant constituents of the TCS, with prominent nuclear enlargement, hyperchromasia, and irregularity (Fig. 1B), and scattered mitotic activity, apoptotic bodies, and even focal necrosis. In some areas the immature neuroepithelial tissue had a striking clear cell appearance (Fig. 1C) and prominent rosettes were seen in several cases (Fig. 1D) with morphology that overlapped with glands. More mature areas displayed abundant neurofibrillary stroma (Fig. 1E) and frequently had a nested appearance with intermixed ganglion-like cells (Fig. 1F).

The mesenchymal elements were the second-most common component of the TCS, and were the dominant constituent in 7 cases (28%). All cases had sheets and fascicles of undifferentiated spindle cells that ranged from markedly hypercellular zones that merged with the primitive neuroepithelial elements (Fig. 2A) to strikingly paucicellular foci that were difficult to recognize as tumor (Fig. 2B); these cells were embedded in varying amounts of fibrous to myxoid stroma. However, components with well-developed heterologous differentiation were present in a subset of tumors. Five cases (20%) had rhabdomyoblastic elements, with prominent strap cells with abundant eosinophilic, striated cytoplasm (Fig. 2C), while 2 cases (8%) showed smooth muscle differentiation with elongated nuclei and pale eosinophilic cytoplasm (Fig. 2D). There were also 4 (16%) cases with mature bone formation (Fig. 2E) and 2 cases (8%) with immature cartilage (Fig. 2F).

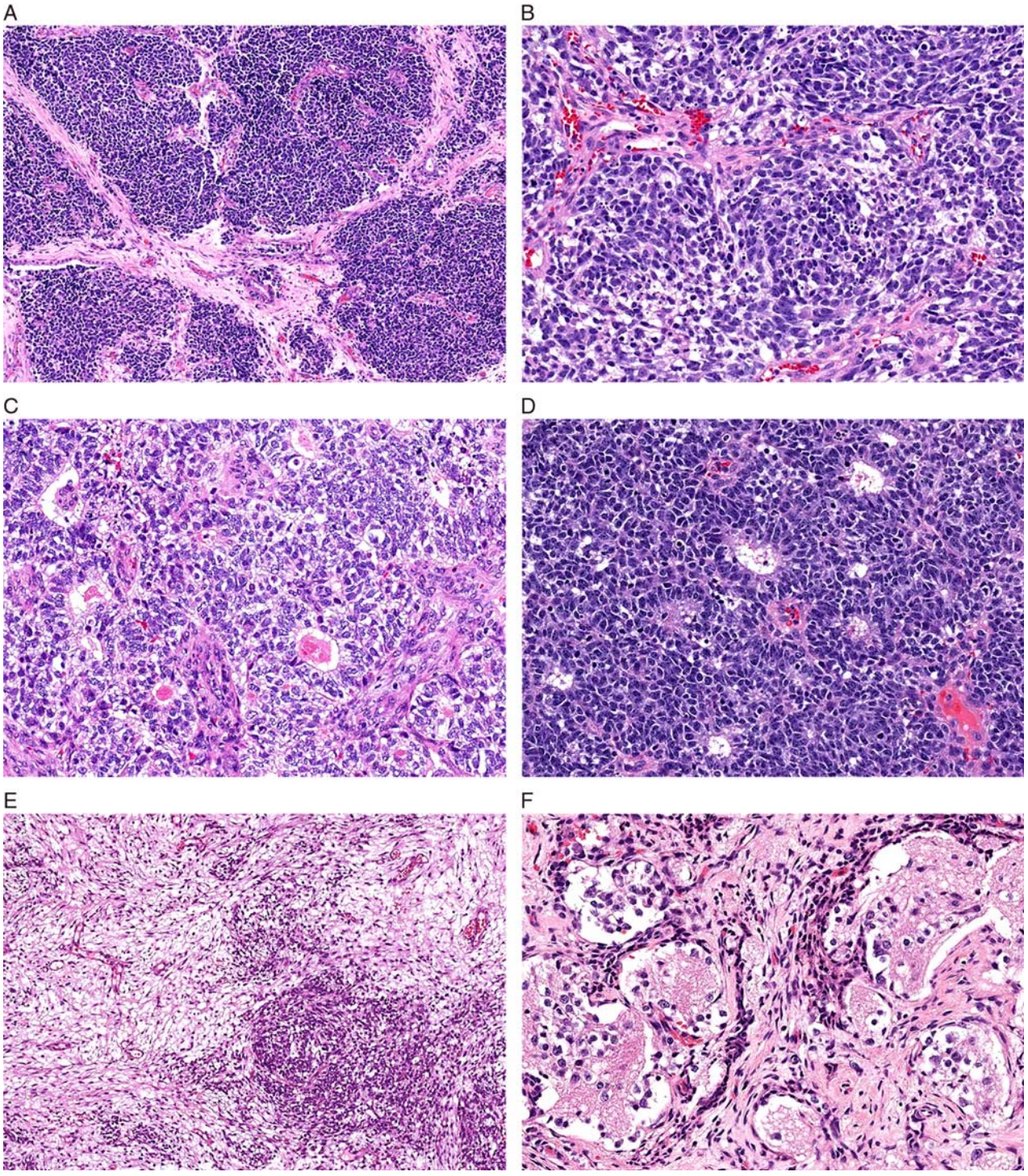

FIGURE 1. All TCS included nests and sheets of immature neuroepithelial cells (A) that had an overtly malignant appearance including large, hyperchromatic, and angulated nuclei (B). These primitive neuroepithelial elements showed occasional areas of clear cell change (C) with frequent prominent rosettes (D). A subset of TCS showed more mature neural elements that had prominent neurofibrillary stroma (E) and often displayed nested architecture with ganglion-like cells (F).

The epithelial elements were the least common constituent of the TCS and comprised the dominant component in only 2 cases (8%). Squamous and glandular differentiation were seen at nearly equal frequencies, with squamous epithelium in 22 cases (88%) and glands in 21 cases (84%). Almost all squamous elements had abundant cytoplasm with variable cytoplasmic clearing and prominent cell membranes that conferred a fetal appearance (Fig. 3A). Rare cases

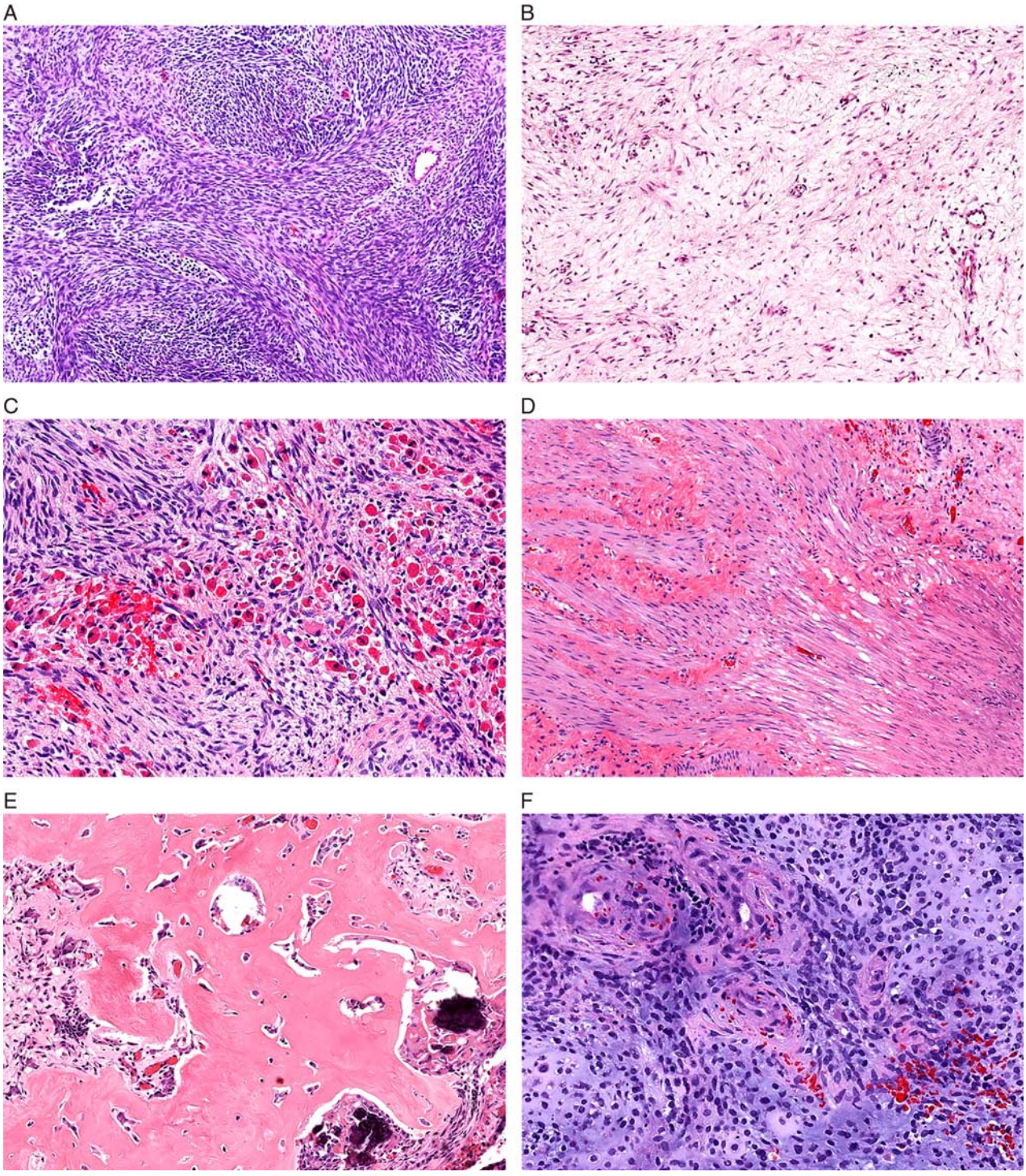

FIGURE 2. All TCS had fascicles of undifferentiated spindle cells that ranged from hypercellular (A) to paucicellular (B). A small subset of cases displayed heterologous differentiation, including rhabdomyoblastic elements with strap cells (C), fascicles of smooth muscle (D), and overt formation of mature bone (E) and immature cartilage (F).

showed abundant anastomosing lobules of squamous epithelium with a papillary pattern (Fig. 3B) or colonization of the surface epithelium that mimicked benign tissue constituents (Fig. 3C). Many glands also displayed a fetal appearance with prominent cytoplasmic clearing (Fig. 3D). However, other glands had prominent mucin production and even displayed rare paneth-like cells (Fig. 3E). Although the epithelium was cytologically bland in most cases, there were rare areas where epithelial components displayed increased cytologic atypia, mitotic activity, and focal necrosis (Fig. 3F).

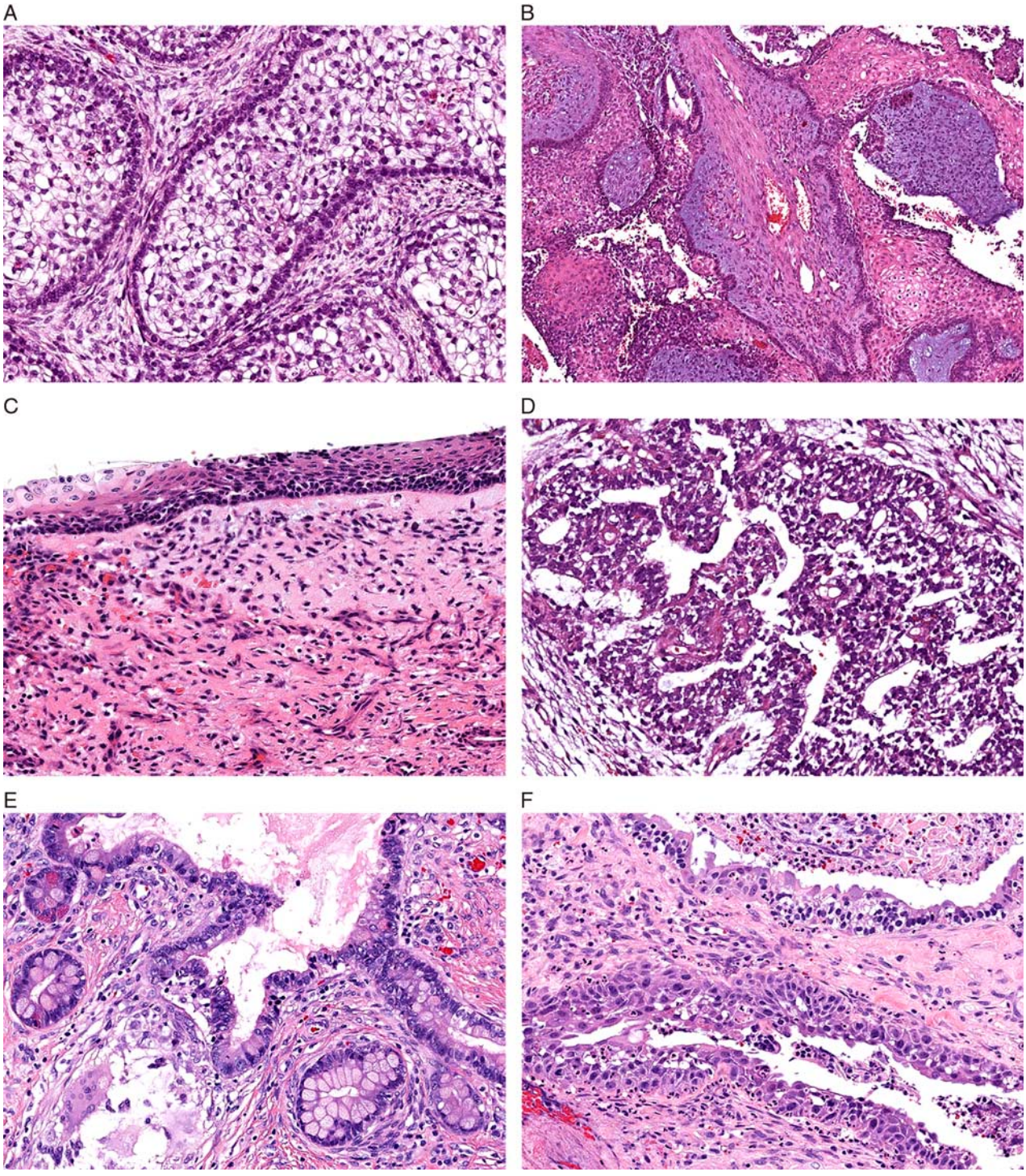

FIGURE 3. The epithelial components of TCS included squamous cells with glycogenated cytoplasm and prominent intracellular borders that conferred a fetal appearance (A) and in rare cases had a papillary pattern (B) or colonized surface epithelium (C). Glands also shared the clear cell fetal appearance (D) or had a highly differentiated mucinous pattern with scattered paneth-like cells (E). Rarely, the epithelial elements displayed increased cytologic atypia and mitotic activity (F).

IHC Findings

SMARCA4 IHC was available for all cases. Across the total cohort there were 22 cases (73%) that showed some degree of SMARCA4 loss, including 18 cases (60%) that showed total loss of IHC expression (Fig. 4A) and 4 cases (13%) that showed partial loss of IHC expression (Fig. 4B). In the cases with partial loss of expression, retained staining was generally seen in the neuroepithelial

and epithelial elements, while the mesenchymal elements displayed diminished expression. Eight cases (27%) had intact SMARCA4 IHC. Tissue was available for SMARCB1 IHC in 19 cases. Although no cases showed total loss of SMARCB1 expression, there were 7 cases (37%) that displayed partial loss (Fig. 4C). Similar to the pattern for SMARCA4, neuroepithelial and epithelial tissues also showed greater SMARCB1 expression in most of these cases. Twelve cases (63%) had intact SMARCB1 IHC expression. Tissue was available for β-catenin IHC in 22 cases. Of these cases, 14 (64%) showed some degree of nuclear localization that ranged from focal to patchy (Fig. 4D). The epithelial elements, particularly foci of squamous differentiation, seemed to most commonly display nuclear β-catenin. Eight cases (36%) had only membranous β-catenin expression, which was not regarded as positive.

Molecular Findings

NGS results are summarized in Figure 5. Overall, there were 11 cases (65%) that demonstrated *SMARCA4* alterations, of which 10 had biallelic inactivation. These alterations included a variety of mechanisms, including frameshift mutation (n = 8), nonsense mutation (n = 6), splice site mutation (n = 3), copy-number loss (n = 2), copy-number gain (n = 1), and missense mutations (n = 1). A total of 6 cases had *CTNNB1* alterations, 5 of which also had *SMARCA4* alterations. All of these cases had activating missense mutations, with an additional biallelic in-frame insertion-deletion in 1 case. Among the 5 cases that did not have either *SMARCA4* or *CTNNB1* mutations, 2 cases had alterations of other genes in the SWI/SNF complex or Wnt pathways, including 1 with both *APC* frameshift mutation and *ARID1A* nonsense mutation and 1 case with *SMARCB1* inactivation including homozygous copy loss. There were also 3 cases which lacked SWI/SNF or Wnt pathway alterations, including 1 case with a *DICER1* hotspot missense mutation and copy-neutral loss of heterozygosity, 1 case with a variety of genetic alterations including biallelic copy-number loss in *MAP3K1* and *RB1*, and 1 case with no identifiable oncogenic alterations. In addition to these presumed oncogenic drivers, numerous additional mutations were seen throughout the cohort, including several mutations in *KMT2A*, *KMT2B*, *KMT2C*, *KMT2D*, *NOTCH1*, *NOTCH3*, and *TP53*. Although RNA sequencing was not performed and would be necessary to entirely rule out gene rearrangements, *NAB2::STAT6* fusion was not identified in any case on manual review of these loci.

Correlation between molecular, IHC, and histologic findings is also depicted in Figure 5. The cohort that underwent NGS was enriched for retained SMARCA4 IHC, including 8 cases with complete SMARCA4 loss (47%), 3 cases with partial loss (18%), and 6 cases with intact expression (35%). Of the 11 cases with *SMARCA4* inactivation, 10 cases (91%) demonstrated some degree of SMARCA4 IHC loss, including 8 cases with total loss and 2 cases with partial loss. Indeed, all cases with total SMARCA4 loss by IHC that underwent NGS had molecular evidence of *SMARCA4* inactivation, 3 of which also had concomitant *CTNNB1* activating mutation. However, SMARCA4 IHC loss was not entirely sensitive for molecular alteration, as 1 case with *SMARCA4* frameshift mutation and copy-number gain maintained full SMARCA4 expression. Both cases with partial SMARCA4 IHC loss in the setting of *SMARCA4* inactivating mutation showed concomitant *CTNNB1* mutation. In addition, 1 case with *CTNNB1* alteration but no *SMARCA4* inactivation did have partial SMARCA4 IHC loss. The 1 case that had *SMARCB1* mutation showed partial SMARCB1 IHC loss, as did 2 other cases with *SMARCA4* mutation. Of the 6 cases with *CTNNB1* mutation, β-catenin IHC was available for 4, 2 of which (50%) showed nuclear localization. Nuclear β-catenin was also present in 75% of cases tested that lacked *CTNNB1* mutation, including 2 cases with *SMARCA4* loss and 1 case with *APC* mutation. Histologically, a predominant neuroepithelial component was most common in cases with *SMARCA4* inactivation (64%), while tumors that lacked *SMARCA4* alterations more commonly had predominant mesenchymal components (67%); however, these differences were not statistically significant (all $P > 0.05$).

DISCUSSION

In the largest molecular analysis of sinonasal TCS performed to date, we confirm that inactivating *SMARCA4* mutations are the predominant genetic event in this tumor type, with rare involvement of other SWI/SNF complex members *SMARCB1* and *ARID1A*. We previously described frequent loss of SMARCA4 in an IHC study of 22 cases of TCS.[8] In this expanded series, which included 8 additional tumors, we identified some degree of SMARCA4 loss by IHC in 73% of cases, including 60% with total loss of expression. This correlated strongly with NGS findings in 17 cases, 65% of which showed molecular evidence of *SMARCA4* inactivation despite the cohort's being enriched for partial or intact IHC expression. Notably, total IHC loss of SMARCA4 was always associated with *SMARCA4* inactivation at the molecular level. However, partial SMARCA4 loss was seen in cases with and without *SMARCA4* mutation, and 1 case with *SMARCA4* mutation had intact IHC expression, possibly due to additional copy-number gain. The absolute proportion of TCS cases with SMARCA4 IHC loss is still unclear, as Kakkar et al[13] recently reported loss of SMARCA4 in just 29% of cases at their center. It is difficult to determine whether this difference reflects nonrepresentative sampling due to relatively small sample sizes, variation across patient populations, or different diagnostic thresholds for TCS. However, the findings in our series do suggest that IHC loss of SMARCA4 does correlate with inactivating *SMARCA4* mutations in a majority of cases. The presence of *SMARCB1* and *ARID1A* mutations in rare cases that lacked *SMARCA4* mutations also indicate a broader role for SWI/SNF complex members in this tumor type.

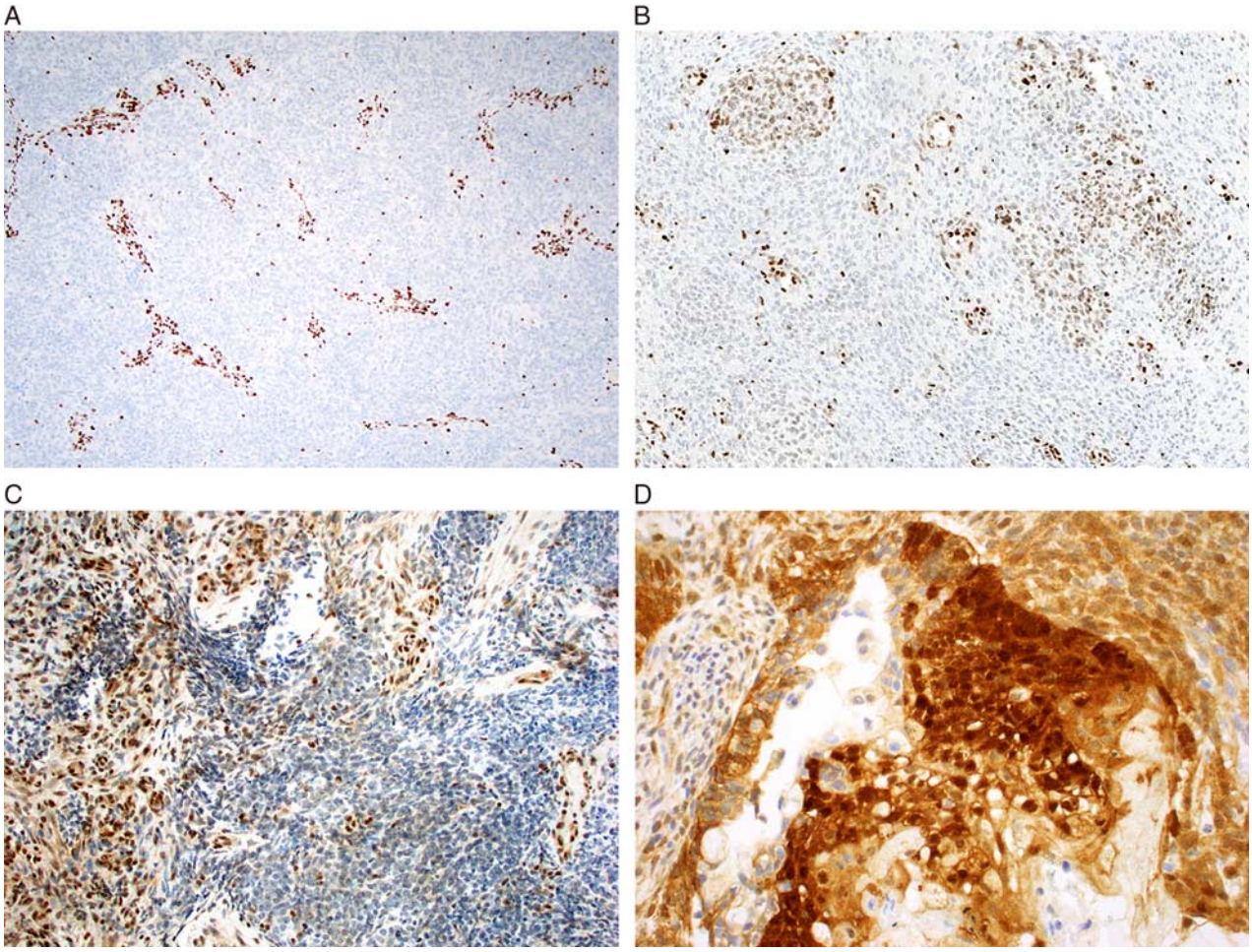

FIGURE 4. Across the entire cohort of TCS, 60% of cases showed total SMARCA4 loss in tumor cells with retained internal control in blood vessels (A), while 13% of cases showed partial loss with the strongest expression in neuroepithelial and epithelial components (B). There was also partial loss of SMARCB1 in 37% of cases tested (C). Focal to patchy nuclear β-catenin localization was seen in 64% of cases, most commonly in epithelial elements (D).

In addition, our results confirm a role for Wnt pathway genes in sinonasal TCS, with recurrent activating *CTNNB1* mutations and rare *APC* alteration. The Wnt pathway is well-established to play a pivotal role in human development and multiple cancer types. Among sinonasal entities, Wnt pathway alterations are most widely recognized in soft tissue tumors, with recurrent *CTNNB1* activating mutations in sinonasal glomangiopericytoma and *CTNNB1* and *APC* mutations in nasopharyngeal angiofibroma.[14,15] Birkeland et al[10] initially described activating *CTNNB1* mutation and nuclear β-catenin expression in 1 case of TCS. In this study, we identified activating *CTNNB1* mutations in 35% of cases, all but one of which were seen in combination with *SMARCA4* mutations. We also identified a mutation in *APC*, another Wnt pathway gene, in a single case in combination with *ARID1A* mutation. Importantly, while nuclear β-catenin was seen by IHC in 64% of TCS, it did not track as closely with *CTNNB1* mutation status as SMARCA4 IHC. Only 50% of cases with *CTNNB1* mutation showed nuclear localization of β-catenin and 75% of cases that lacked *CTNNB1* alteration had some degree of nuclear staining. There is also some variability in β-catenin staining reported across institutions, as Compton et al[16] recently reported no nuclear localization in a small series of TCS. Notably, the Wnt pathway has long been established in laboratory studies to have complex interaction with *SMARCA4*,[17,18] and it is possible that the overlap in these elements leads to the variable staining profiles. Regardless, these results do indicate that activating *CTNNB1* mutations are the second-most common alteration in TCS and suggest that β-catenin may be a valuable tool for confirming the diagnosis in a subset of cases, especially when there is limited material and not all of the histologic features are identified.

These additional molecular findings also serve to highlight that TCS is not restricted to the SWI/SNF complex and Wnt pathways. Notably, 1 case harbored a hotspot mutation in *DICER1*, a gene that regulates miRNA processing and plays an oncogenic role in several

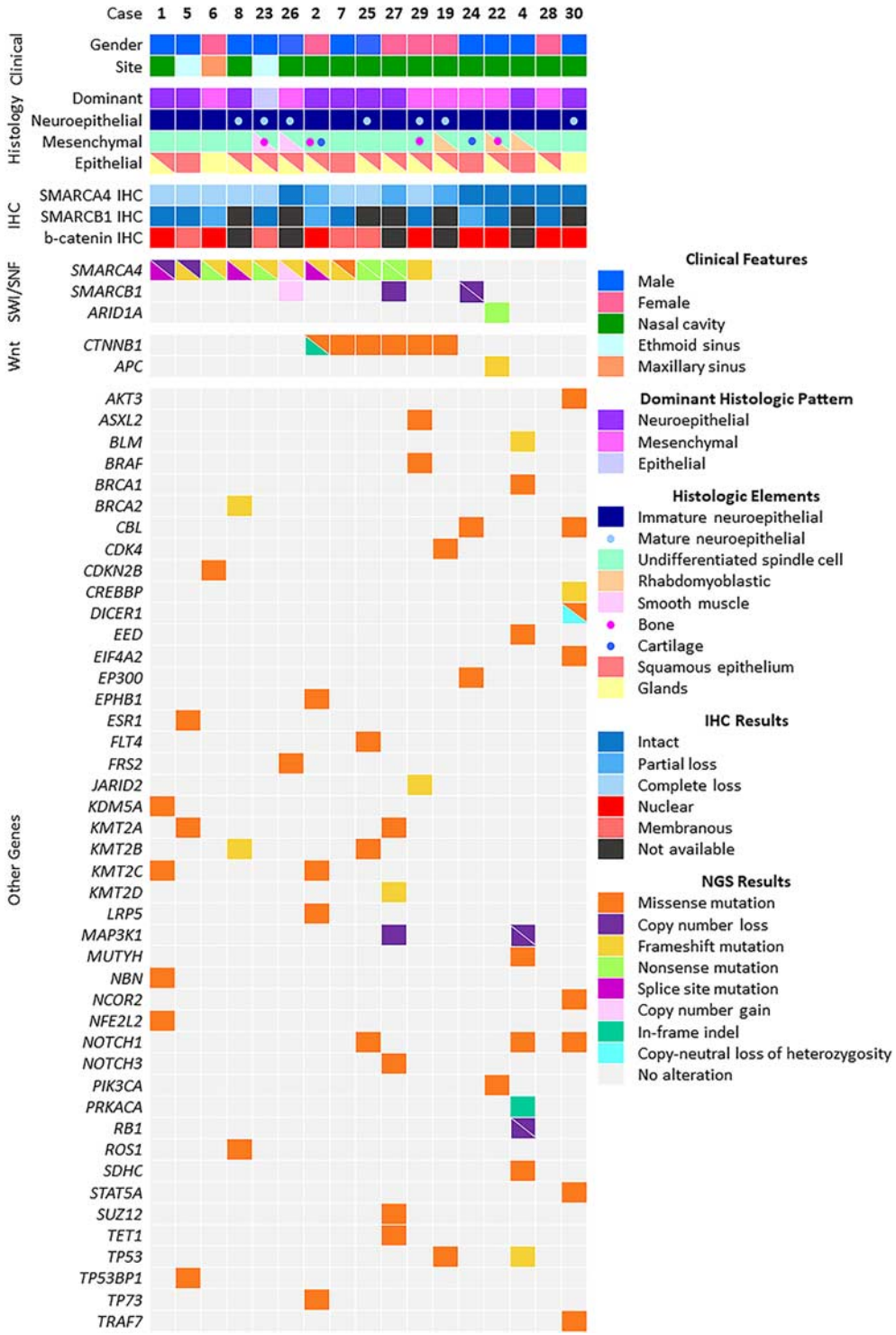

FIGURE 5. Clinical, histologic, IHC, and molecular features of TCS are depicted with cases organized by molecular findings. Biallelic *SMARCA4* inactivation was the most common molecular alteration in TCS and correlated strongly with IHC loss. Activating *CTNNB1* mutations were frequently seen in combination with *SMARCA4* inactivation. Additional molecular drivers included other SWI/SNF complex members *SMARCB1* and *ARID1A* and Wnt pathway constituent *APC* as well as *DICER1*.

malignancies. Interestingly, a significant subset of tumors defined by *DICER1* mutations are notable for multilineage differentiation or primitive neuroepithelial components similar to TCS.[19–26] In the head and neck, recent identification of recurrent *DICER1* mutations allowed for definition of thyroblastoma, a novel category of thyroid

malignancy that includes multilineage tumors previously classified as malignant thyroid teratoma and shows striking histologic resemblance to TCS.[27,28] Rare interchangeability between *SMARCA4* and *DICER1* has also been previously documented, with 1 case of a pleuropulmonary blastoma-like neoplasm in an infant showing *SMARCA4* inactivation instead of *DICER1* mutation.[29] We also identified a *PIK3CA* hotspot mutation in 1 case, similar to what was reported by Belardinilli et al,[9] but this alteration was present in combination with *APC* and *ARID1A* mutations, and it is unclear if this gene has a unique role in TCS. Additional cases of TCS showed a nonspecific constellation of molecular alterations or no clear oncogenic drivers. However, regardless of molecular underpinnings, all cases were histologically indistinguishable from cases with SWI/SNF complex and Wnt pathway mutations.

All of these molecular findings add to evidence that sinonasal TCS is related to sinonasal carcinomas that show neuroendocrine or neuroectodermal differentiation. Before recognition as a separate entity, most SMARCA4-deficient sinonasal carcinomas were classified as high-grade neuroendocrine carcinoma, with large cell or, less frequently, small cell histologic patterns and weak synaptophysin positivity.[30,31] The small cell pattern in particular closely overlaps with the often-dominant neuroepithelial components of TCS. The presence of recurrent *SMARCA4* inactivation at a molecular level in TCS in combination with these histologic and IHC similarities cements the relationship between TCS and SMARCA4-deficient sinonasal carcinomas. Of course, other sinonasal tumors still regarded as high-grade neuroendocrine carcinoma also bear histologic and IHC similarity to the immature neuroepithelial tissue in TCS. Interestingly, Dogan et. al also documented that several such tumors also have SWI/SNF and Wnt pathway alterations, with recurrent *ARID1A*, *CTNNB1*, *AMER1*, and *APC* mutations identified in tumors described as small cell carcinoma and poorly differentiated carcinoma with neuroendocrine and glandular features.[32] These findings suggest that TCS may have a broader relationship to sinonasal neuroendocrine neoplasms.

While these results substantially clarify the pathogenesis of sinonasal TCS, they also indicate that this tumor should not be a molecularly defined entity. In the last decade, recognition of recurrent oncogenic drivers has allowed for definition of several novel tumor types and subtypes in the sinonasal tract, including SMARCB1-deficient sinonasal carcinoma, SMARCA4-deficient sinonasal carcinoma, human papillomavirus–related multiphenotypic sinonasal carcinoma, and *DEK::AFF2* carcinoma.[30,31,33–41] However, all of these tumors not only have definitional genetic findings but also recognizable morphologic and IHC features that support their uniqueness. Moreover, other sinonasal tumors, including squamous cell carcinoma, intestinal-type adenocarcinoma, and non–intestinal-type adenocarcinoma, harbor substantial molecular variability despite well-defined histologic features.[35,42–45] Regardless of their heterogenous genetic underpinnings, all TCS in this series fell within a discrete histologic spectrum with the diagnostic neuroepithelial, epithelial, and mesenchymal components. As such, molecular testing should not be regarded as necessary to make a TCS diagnosis. On a similar level, both SMARCA4 and β-catenin IHC are potentially useful diagnostic adjuncts in cases with limited material or when not all histologic patterns are present. However, neither of these stains are entirely sensitive or specific for a diagnosis of TCS or even corresponding molecular alterations and should not be considered a requisite part of the diagnosis.

In summary, this study confirms a dominant role for *SMARCA4* inactivation in sinonasal TCS that correlates strongly with loss of IHC expression. It also highlights recurrent activating *CTNNB1* mutations and common β-catenin nuclear expression. However, it illustrates that some cases of TCS display alternate genetic alterations, most notably including a single case with *DICER1* hotspot mutation. Future accumulation of larger series of TCS with more extensive follow-up data will be necessary to determine the clinical significance of these various molecular alterations. Nevertheless, these findings solidify the link between sinonasal TCS and SMARCA4-deficient sinonasal carcinoma and other sinonasal carcinomas that display neuroendocrine differentiation. Furthermore, they also strongly suggest that sinonasal TCS should not be considered a molecularly defined diagnosis.

REFERENCES

1. Rooper LM, Agaimy A, Bal MM, et al. Teratocarcinosarcoma. In: WHO Classification of Tumours Editorial Board, ed. *WHO Classification of Head and Neck Tumours*. Lyon, France: International Agency for Research on Cancer; 2022.
2. Franchi A, Wenig BM. Teratocarcinosarcoma. In: Lloyd RV, Osamura RY, Kloppel G, et al, eds. *WHO Classification of Tumours of Endocrine Organs*. Lyon, France: International Agency for Research on Cancer; 2017:26–27.
3. Heffner DK, Hyams VJ. Teratocarcinosarcoma (malignant teratoma?) of the nasal cavity and paranasal sinuses: a clinicopathologic study of 20 cases. *Cancer*. 1984;53:2140–2154.
4. Pai SA, Naresh KN, Masih K, et al. Teratocarcinosarcoma of the paranasal sinuses: a clinicopathologic and immunohistochemical study. *Hum Pathol*. 1998;29:718–722.
5. Salem F, Rosenblum MK, Jhanwar SC, et al. Teratocarcinosarcoma of the nasal cavity and paranasal sinuses: report of 3 cases with assessment for chromosome 12p status. *Hum Pathol*. 2008;39:605–609.
6. Shanmugaratnam K, Kunaratnam N, Chia KB, et al. Teratoid carcinosarcoma of the paranasal sinuses. *Pathology*. 1983;15:413–419.
7. Thomas J, Adegboyega P, Iloabachie K, et al. Sinonasal teratocarcinosarcoma with yolk sac elements: a neoplasm of somatic or germ cell origin? *Ann Diagn Pathol*. 2011;15:135–139.
8. Rooper LM, Uddin N, Gagan J, et al. Recurrent loss of SMARCA4 in sinonasal teratocarcinosarcoma. *Am J Surg Pathol*. 2020;44:1331–1339.
9. Belardinilli F, De Vincentiis L, D'Ecclesia A, et al. PIK3CA somatic mutation in sinonasal teratocarcinosarcoma. *Auris Nasus Larynx*. 2021;48:530–534.
10. Birkeland AC, Burgin SJ, Yanik M, et al. Pathogenetic analysis of sinonasal teratocarcinosarcomas reveal actionable beta-catenin overexpression and a beta-catenin mutation. *J Neurol Surg B Skull Base*. 2017;78:346–352.
11. Stevens TM, Rooper LM, Bacchi CE, et al. Teratocarcinosarcoma-like and adamantinoma-like head and neck neoplasms harboring NAB2::STAT6: unusual variants of solitary fibrous tumor or novel tumor entities? *Head Neck Pathol*. 2022;16:746–754.

12. Bishop JA, Gagan J, Baumhoer D, et al. Sclerosing polycystic "Adenosis" of salivary glands: a neoplasm characterized by PI3K pathway alterations more correctly named sclerosing polycystic adenoma. *Head Neck Pathol*. 2020;14:630–636.
13. Kakkar A, Ashraf SF, Rathor A, et al. SMARCA4/BRG1-deficient sinonasal carcinoma: morphologic spectrum of an evolving entity. *Arch Pathol Lab Med*. 2021;146:1122–1130.
14. Agaimy A, Haller F. CTNNB1 (beta-Catenin)-altered neoplasia: a review focusing on soft tissue neoplasms and parenchymal lesions of uncertain histogenesis. *Adv Anat Pathol*. 2016;23:1–12.
15. Lasota J, Felisiak-Golabek A, Aly FZ, et al. Nuclear expression and gain-of-function beta-catenin mutation in glomangiopericytoma (sinonasal-type hemangiopericytoma): insight into pathogenesis and a diagnostic marker. *Mod Pathol*. 2015;28:715–720.
16. Compton ML, Lewis JS Jr, Faquin WC, et al. SALL-4 and beta-catenin expression in sinonasal teratocarcinosarcoma. *Head Neck Pathol*. 2022;16:229–235.
17. Barker N, Hurlstone A, Musisi H, et al. The chromatin remodelling factor Brg-1 interacts with beta-catenin to promote target gene activation. *EMBO J*. 2001;20:4935–4943.
18. Vasileiou G, Ekici AB, Uebe S, et al. Chromatin-remodeling-factor ARID1B represses wnt/beta-catenin signaling. *Am J Hum Genet*. 2015;97:445–456.
19. Hill DA, Ivanovich J, Priest JR, et al. DICER1 mutations in familial pleuropulmonary blastoma. *Science*. 2009;325:965.
20. Pugh TJ, Yu W, Yang J, et al. Exome sequencing of pleuropulmonary blastoma reveals frequent biallelic loss of TP53 and two hits in DICER1 resulting in retention of 5p-derived miRNA hairpin loop sequences. *Oncogene*. 2014;33:5295–5302.
21. Sahm F, Jakobiec FA, Meyer J, et al. Somatic mutations of DICER1 and KMT2D are frequent in intraocular medulloepitheliomas. *Genes Chromosomes Cancer*. 2016;55:418–427.
22. Stewart DR, Messinger Y, Williams GM, et al. Nasal chondromesenchymal hamartomas arise secondary to germline and somatic mutations of DICER1 in the pleuropulmonary blastoma tumor predisposition disorder. *Hum Genet*. 2014;133:1443–1450.
23. de Kock L, Sabbaghian N, Druker H, et al. Germ-line and somatic DICER1 mutations in pineoblastoma. *Acta Neuropathol*. 2014;128:583–595.
24. de Kock L, Sabbaghian N, Plourde F, et al. Pituitary blastoma: a pathognomonic feature of germ-line DICER1 mutations. *Acta Neuropathol*. 2014;128:111–122.
25. Priest JR, Williams GM, Manera R, et al. Ciliary body medulloepithelioma: four cases associated with pleuropulmonary blastoma—a report from the International Pleuropulmonary Blastoma Registry. *Br J Ophthalmol*. 2011;95:1001–1005.
26. McCluggage WG, Stewart CJR, Belcijan NL, et al. Neuroectodermal elements are part of the morphological spectrum of DICER1-associated neoplasms. *Hum Pathol*. 2022;123:46–58.
27. Agaimy A, Witkowski L, Stoehr R, et al. Malignant teratoid tumor of the thyroid gland: an aggressive primitive multiphenotypic malignancy showing organotypical elements and frequent DICER1 alterations—is the term "thyroblastoma" more appropriate? *Virchows Arch*. 2020;477:787–798.
28. Rooper LM, Bynum JP, Miller KP, et al. Recurrent DICER1 hotspot mutations in malignant thyroid gland teratomas: molecular characterization and proposal for a separate classification. *Am J Surg Pathol*. 2020;44:826–833.
29. de Kock L, Fahiminiya S, Fiset PO, et al. Infantile pulmonary teratoid tumor. *N Engl J Med*. 2018;378:2238–2240.
30. Agaimy A, Jain D, Uddin N, et al. SMARCA4-deficient sinonasal carcinoma: a series of 10 cases expanding the genetic spectrum of SWI/SNF-driven sinonasal malignancies. *Am J Surg Pathol*. 2020;44:703–710.
31. Agaimy A, Weichert W. SMARCA4-deficient sinonasal carcinoma. *Head Neck Pathol*. 2017;11:541–545.
32. Dogan S, Vasudevaraja V, Xu B, et al. DNA methylation-based classification of sinonasal undifferentiated carcinoma. *Mod Pathol*. 2019;32:1447–1459.
33. Agaimy A, Daum O, Markl B, et al. SWI/SNF complex-deficient undifferentiated/rhabdoid carcinomas of the gastrointestinal tract: a series of 13 cases highlighting mutually exclusive loss of SMARCA4 and SMARCA2 and frequent co-inactivation of SMARCB1 and SMARCA2. *Am J Surg Pathol*. 2016;40:544–553.
34. Bishop JA, Hang JF, Kiss K, et al. HPV-related multiphenotypic sinonasal carcinoma. In: WHO Classification of Tumours Editorial Board, ed. *WHO Classification of Head and Neck Tumours*. Lyon, France: International Agency for Research on Cancer; 2022.
35. Rooper LM, Ihrler S, Kiss K, et al. Non-keratinizing squamous cell carcinoma. In: WHO Classification of Tumours Editorial Board, ed. *WHO Classification of Head and Neck Tumours*. Lyon, France: International Agency for Research on Cancer; 2022.
36. Agaimy A, Hartmann A, Antonescu CR, et al. SMARCB1 (INI-1)-deficient sinonasal carcinoma: a series of 39 cases expanding the morphologic and clinicopathologic spectrum of a recently described entity. *Am J Surg Pathol*. 2017;41:458–471.
37. Agaimy A, Koch M, Lell M, et al. SMARCB1(INI1)-deficient sinonasal basaloid carcinoma: a novel member of the expanding family of SMARCB1-deficient neoplasms. *Am J Surg Pathol*. 2014;38:1274–1281.
38. Bishop JA, Antonescu CR, Westra WH. SMARCB1 (INI-1)-deficient carcinomas of the sinonasal tract. *Am J Surg Pathol*. 2014;38:1282–1289.
39. Kuo YJ, Lewis JS Jr, Zhai C, et al. DEK-AFF2 fusion-associated papillary squamous cell carcinoma of the sinonasal tract: clinicopathologic characterization of seven cases with deceptively bland morphology. *Mod Pathol*. 2021;34:1820–1830.
40. Rooper LM, Agaimy A, Dickson BC, et al. DEK-AFF2 carcinoma of the sinonasal region and skull base: detailed clinicopathologic characterization of a distinctive entity. *Am J Surg Pathol*. 2021;45:1682–1693.
41. Todorovic E, Truong T, Eskander A, et al. Middle ear and temporal bone nonkeratinizing squamous cell carcinomas with DEK-AFF2 fusion: an emerging entity. *Am J Surg Pathol*. 2020;44:1244–1250.
42. Bell D, Jain D, Sandison A, et al. Keratinizing squamous cell carcinoma. In: WHO Classification of Tumours Editorial Board, ed. *WHO Classification of Head and Neck Tumours*. Lyon, France: International Agency for Research on Cancer; 2022.
43. Stelow EB, Laco J, Leivo I, et al. Non-intestinal type sinonasal adenocarcinoma. In: WHO Classification of Tumours Editorial Board, ed. *WHO Classification of Head and Neck Tumours*. Lyon, France: International Agency for Research on Cancer; 2022.
44. Franchi A, Leivo I, Patil A, et al. Intestinal-type sinonasal adenocarcinoma. In: WHO Classification of Tumours Editorial Board, ed. *WHO Classification of Head and Neck Tumours*. Lyon, France: International Agency for Research on Cancer; 2022.
45. Rooper LM, Thompson LDR, Gagan J, et al. Low-grade non-intestinal-type sinonasal adenocarcinoma: a histologically distinctive but molecularly heterogeneous entity. *Mod Pathol*. 2022;35:1160–1167.